

Directly Observable Speed of Optical Precursors

Chuan-Feng Li,^{1*} Zong-Quan Zhou,¹ Heejeong Jeong,² and Guang-Can Guo¹

¹Key Laboratory of Quantum Information, University of Science and Technology of China, CAS, Hefei, 230026, People's Republic of China

²Thayer School of Engineering, Dartmouth College, Hanover, New Hampshire, 03755, USA

(Dated: December 2, 2024)

Precursors can serve as a bound on the speed of information with dispersive medium. We propose a method to identify the speed of optical precursors using polarization-based interference in a solid-state device, which can bound the accuracy of the precursors' speed to less than 10^{-4} with conventional experimental conditions. Our proposal may have important implications for optical communications and fast information processing.

PACS numbers: 42.50.Gy 42.25.Bs 03.30.+p

Velocity of light has been of research interest for more than 100 years because it is directly related to the causality through Einstein's special theory of relativity [1]. Unlike the well defined velocity of a point particle, the velocity of a light pulse traveling through an optical material is not precisely defined. The motion of a light pulse can be approximated by the group velocity (v_g), which is given by $v_g = c/(n + \omega dn/d\omega)$, where c is the speed of light in a vacuum, n is the refractive index of the material and ω is the frequency of the light [2]. It can be clearly seen that v_g can be greater than c and even be negative when $\omega dn/d\omega$ is negative (anomalous dispersion). Experimental studies of fast light propagation include [3–7]. To resolve the apparent contradictions between fast light propagation and the theory of relativity, optical precursors were introduced by Sommerfeld and Brillouin in 1914 [8–10]. The theory states that the front edges of a step modulated pulse propagate at the speed c because of the finite response time of any physical material and no components can overtake this wavefront. The forerunners, now known as Sommerfeld-Brillouin precursors, are followed by the main pulse traveling at its group velocity. This conclusion, while conceptually clear, lacks of experimental evidence directly relating to the speed of optical precursors.

Optical precursors are recently of great interest because they have applications in biomedical imaging [11], underwater communications [12] and the generation of high peak power optical pulses [13, 14]. A number of theoretical and experimental studies have been carried out [15–20]. Specifically, direct observation of precursors which are separated from the delayed main fields have been achieved with electromagnetically induced transparency (EIT) in cold atoms [20]. For all these experiments, the authors claim that the rising edge of the input pulse propagates at the speed of c in the form of Sommerfeld precursor. However, considering the rise time of the detecting systems, a time delay of shorter than 1 ps would not be captured if the precursors travel at a speed which differs little from c .

In this Letter, we first propose an experimental method to precisely determine the speed of optical precursors propagat-

ing through an EIT medium: optically pumped $\text{Nd}^{3+}:\text{YVO}_4$ crystal. We utilize the fact that the polarization is preserved in precursors right after traveling in different materials. If there is any speed difference between them, the interference pattern will be significantly altered and reveal the speed of the precursors.

$\text{Nd}^{3+}:\text{YVO}_4$ crystals (doping level, 10 p.p.m.) have been systematically investigated as a candidate solid state quantum memory [21–23]. The ${}^4I_{9/2} \rightarrow {}^4F_{3/2}$ transition of Nd^{3+} around 879.705 nm has a narrow homogenous linewidth ($\Gamma_h \sim 63$ kHz) and wideband inhomogeneous broadening ($\Gamma_{inh} \sim 2.1$ GHz) at low temperature. Nd^{3+} is a Kramers ion, and thus has strong first-order Zeeman effect, which yields a large ground state splitting under the application of a magnetic field (10~100 GHz/T). From the inset of Fig. 1(a), it can be seen that a moderate magnetic field splits the ground states into two Zeeman spin levels ($|1\rangle, |2\rangle$) which connect to an excited state ($|3\rangle$). Thus, this provides a Λ -like system [22, 23].

Note that for the rising edge produced by electro-optic modulator (EOM), the pure YVO_4 crystal behaves as a wide band response medium, similar to a window or waveplate that can directly transmit the square pulse. However, the optically pumped Nd^{3+} ions have a narrow band response and strong dispersion for the input pulse. The detectable wave fronts should propagate at the same speed v_0 in both a $\text{Nd}^{3+}:\text{YVO}_4$ crystal and a pure YVO_4 crystal according to Sommerfeld's theory. $v_0 = c/n_0$, n_0 is the refractive index of YVO_4 crystal at 879.705 nm for light polarized parallel to the crystal's symmetric c axis.

The frequency of the probe light is tuned to the Nd^{3+} absorption line (ω_{31}). It is a square pulse modulated using an EOM with a temporal width of t_0 and a rising (falling) time of t_r . The input light intensity is assumed to be one in the following calculations. $E(0, \omega)$ is the Fourier transform of the input pulse. The $\text{Nd}^{3+}:\text{YVO}_4$ crystal undergoing EIT is characterized by its linear susceptibility [24]

$$\chi_1(\omega) = \frac{\alpha_0}{k_0} \frac{4(\Delta + i\gamma_{12})\delta_1}{|\Omega_c|^2 - 4(\Delta + i\gamma_{12})(\Delta + i\delta_1)}, \quad (1)$$

where $\alpha_0 = 4130 \text{ m}^{-1}$ is the on-resonance absorption coefficient; $k_0 = n_0\omega_{31}/c = 1.55 \times 10^7 \text{ m}^{-1}$; $\Delta = \omega - \omega_{31}$ is the probe detuning; and Ω_c is the coupling laser Rabi frequency. $2\delta_1$ is the original absorption bandwidth, which

*email: cfli@ustc.edu.cn

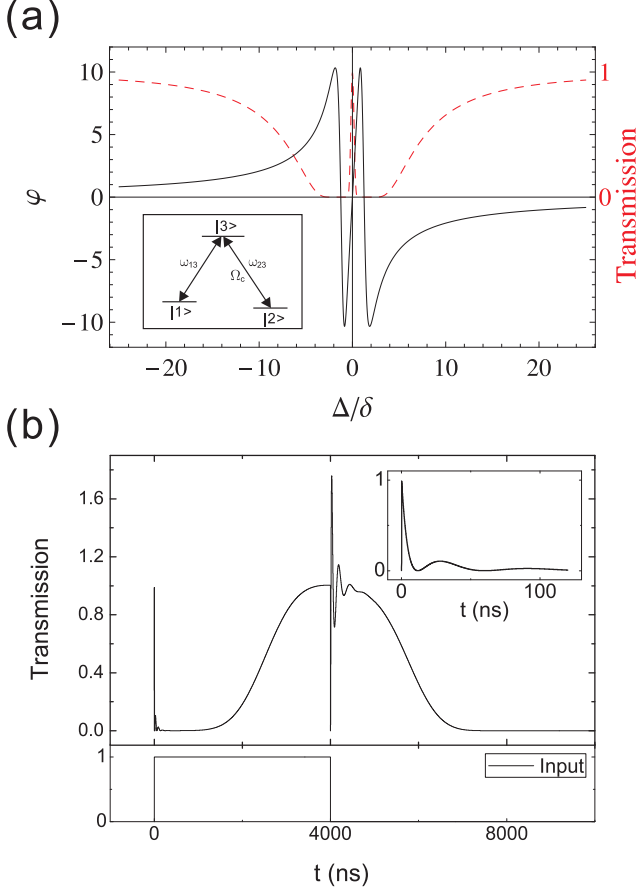


FIG. 1: (color online). (a) The phase (black solid line) and intensity (red dashed line) for light passing through a $\text{Nd}^{3+}:\text{YVO}_4$ crystal versus the probe detuning. The inset is energy level diagram of the $^4I_{9/2} \rightarrow ^4F_{3/2}$ transition of Nd^{3+} under a magnetic field. (b) The transmission of a square pulse passing through a 0.01 m long $\text{Nd}^{3+}:\text{YVO}_4$ crystal. The input square pulse is shown at the bottom as a reference.

is controlled by the pumping procedure. Here, we choose $\delta_1 = 2\pi \times 1$ MHz which is larger than Γ_h and the laser linewidth. The dephasing rate between the two ground states is $\gamma_{12} = 2\pi \times 0.2$ kHz. These parameters were chosen based on experimental observations [22, 23]. The transmitted field is given by $E(z_1, \omega) = E(0, \omega) \text{Exp}[ik_1(\omega)z_1]$ with $k_1(\omega) = k_0 \sqrt{1 + \chi_1(\omega)} \simeq k_0(1 + \chi_1(\omega)/2)$. Via a fast Fourier transformation (FFT), the transmitted field in time domain can be obtained. There have been some analytical solutions to this problem [19], which fit well with the results obtained using the FFT. However, to preserve the phase of the field for the coming interference experiments, we use FFT to evaluate the integrals. Fig. 1(a) shows the phase the photons experiencing $\varphi = \text{Re}[k_1(\omega)z_1] - k_0z_1$ with $z_1 = 0.01$ m and transmitted-field intensity of $\text{Exp}[-2\text{Im}[k_1(\omega)z_1]]$. The coupling light is on-resonance with ω_{32} and renders the medium transparent at the probe resonance frequency. It can be seen that far-detuned light experiences a smaller phase shift than the near-resonance

light. Fig. 1(b) shows the transmission of an input pulse of $t_0 = 4 \times 10^{-6}$ s and $t_r = 0.1 \times 10^{-9}$ s. The oscillations in the rising and falling edge are because of the beating between the two sidebands of the pulse spectrum propagating through optically thick medium. The falling edge has an intensity greater than that of the input pulse because of constructive interference between the delayed main fields and precursors [20]. The rising and falling edge at $t = 0$ and $t = t_0$ do not experience group delay. However, the main fields are approximately delayed by $t_g = 2\alpha_0 z_1 \delta_1 / |\Omega_c|^2 = 2.1 \times 10^{-6}$ s.

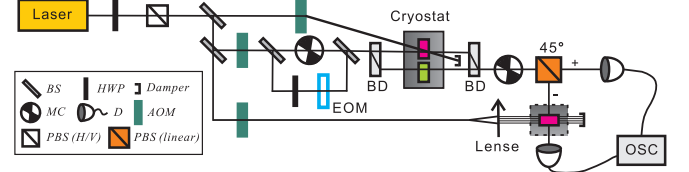


FIG. 2: (color online). Experimental setup for measuring the speed of optical precursors. The coupling light produced by the top AOM should overlap with the probe light in the first $\text{Nd}^{3+}:\text{YVO}_4$ crystal (top, red filled) and be damped then. The pump light for the first $\text{Nd}^{3+}:\text{YVO}_4$ crystal is produced by the middle of the AOM and it is controlled by a MC. The input pulse is produced by the EOM. The lower AOM produce the pump light for the filter. The pure YVO_4 crystal (bottom, green filled) is used as a reference path. After passing through the BD, the light undergoes polarization-dependent detection which is recorded on an oscilloscope (OSC). The MC before the PBS is used to protect the filter and detectors during the pumping procedure of the first $\text{Nd}^{3+}:\text{YVO}_4$ crystal.

The experimental scheme is shown in Fig. 2. The laser should be wavelength tunable and have a linewidth well-below 1 MHz. Using a polarization beam splitter (PBS), and a half wave plate (HWP), the light's polarization can be tuned to maximal absorption for $\text{Nd}^{3+}:\text{YVO}_4$ crystal. The top acousto-optical modulators (AOM) shift the laser frequency to be on resonance with ω_{23} to serve as the coupling light. The middle of the AOM sweep of the laser frequency around ω_{13} serves as the pump light. A mechanical chopper (MC) turns the pump light off during the detection cycle. The input pulse is generated using a 15 GHz EOM and the light's polarization rotated to $|+\rangle = \frac{1}{\sqrt{2}}(|H\rangle + |V\rangle)$ by the HWP, where H and V denote horizontal and vertical polarization state. To show that the precursors actually do travel at the speed of v_0 independently of the Nd^{3+} ions, we use a reference pulse traveling through a pure YVO_4 crystal. The beam displacer (BD) separates H and V polarized light. The H polarized probe light is sent through the $\text{Nd}^{3+}:\text{YVO}_4$ crystal (top, red filled) such that it overlaps with coupling light at a small angle. The V polarized probe light is sent through the pure YVO_4 crystal (bottom, green filled) of the same length z_1 . The $\text{Nd}^{3+}:\text{YVO}_4$ crystal's c axis is aligned in the horizontal direction and YVO_4 crystal's c axis is aligned in the vertical direction to avoid birefringence. All of the crystals are placed in a cryostat with a temperature ~ 3 K and a magnetic field ~ 0.5 T. Then H and V polarized light are combined using the BD and then undergo polarization de-

pendent detection. The transmitted light intensities for the $|+\rangle$ and $|-\rangle = \frac{1}{\sqrt{2}}(|H\rangle - |V\rangle)$ polarizations are recorded using an oscilloscope (OSC). The intensities are given by

$$I_+(z_1, t) = |IFT\{\frac{1}{\sqrt{2}}[E_H(z_1, \omega) + E_V(z_1, \omega)]\}|^2 \quad (2)$$

$$I_-(z_1, t) = |IFT\{\frac{1}{\sqrt{2}}[E_H(z_1, \omega) - E_V(z_1, \omega)]\}|^2, \quad (3)$$

where

$$E_H(z_1, \omega) = \sqrt{1/2}E(0, \omega)Exp[ik_1(\omega)z_1], \quad (4)$$

$$E_V(z_1, \omega) = \sqrt{1/2}E(0, \omega)Exp[ik_0z_1] \quad (5)$$

and IFT means Inverse Fourier Transformation.

To totally eliminate the main fields with the central frequency components, which experience greater phase shifts, another $\text{Nd}^{3+}:\text{YVO}_4$ crystal with the length z_2 is placed before the detectors for $|-\rangle$ polarized light. The crystal's c axis is aligned in the -45° direction for maximal absorption. It acts as a strong absorption filter which can be characterized by

$$\chi_2(\omega) = \frac{\alpha_0}{k_0} \frac{\delta_2}{-(\Delta + i\delta_2)}. \quad (6)$$

This is the special case of Eq. 2 with $\Omega_c = 0$. δ_2 is controlled by the pump light produced by the lower AOM in Fig. 2. In the following text, we refer to this $\text{Nd}^{3+}:\text{YVO}_4$ crystal ‘‘filter’’ for simplicity. With the filter present, the recorded intensity for I_- is given by

$$I_-(z_2, t) = |IFT\{\frac{1}{\sqrt{2}}[E_H(z_1, \omega) - E_V(z_1, \omega)]e^{ik_2(\omega)z_2}\}|^2, \quad (7)$$

where $k_2(\omega) \simeq k_0(1 + \chi_2(\omega)/2)$.

To show the advantages of having the filter present, the simulation results are shown in Fig. 3 with $z_1 = 0.01$ m, $z_2 = 0$ for (a) and $z_1 = 0.01$ m, $z_2 = 0.01$ m for (b). The input pulse is the same as that in Fig. 1 and δ_2 was chosen to be $150\delta_1$. For Fig. 3(a), we first note that the V polarized light remain the same as input square pulse after traveling in pure YVO_4 crystal as mentioned above. When the H polarized precursors decay, the V polarized light starts to dominate. Therefore, I_+ (black solid line) and I_- (red dashed line) have nearly the same intensity. Then, the H polarized main fields slowly increase. I_+ rises with it and I_- decays, because the delayed main fields are still almost entirely in phase with the V polarized light. After 4 μs , V polarized pulse ends, and I_+ and I_- share exactly the same intensities. It can be seen that I_+ rises immediately after $t=0$, but I_- is suppressed during the first nanosecond, because the H polarized precursors experience little phase difference from those of the V polarized photons transmitted through the pure YVO_4 crystal. This shows that H polarized precursors travel at the same speed as the V polarized light in the pure YVO_4 crystal. If this were not the case, I_- would rise at the same time and with the same intensity as I_+ , because only H (V) polarized light presented and there was no interference

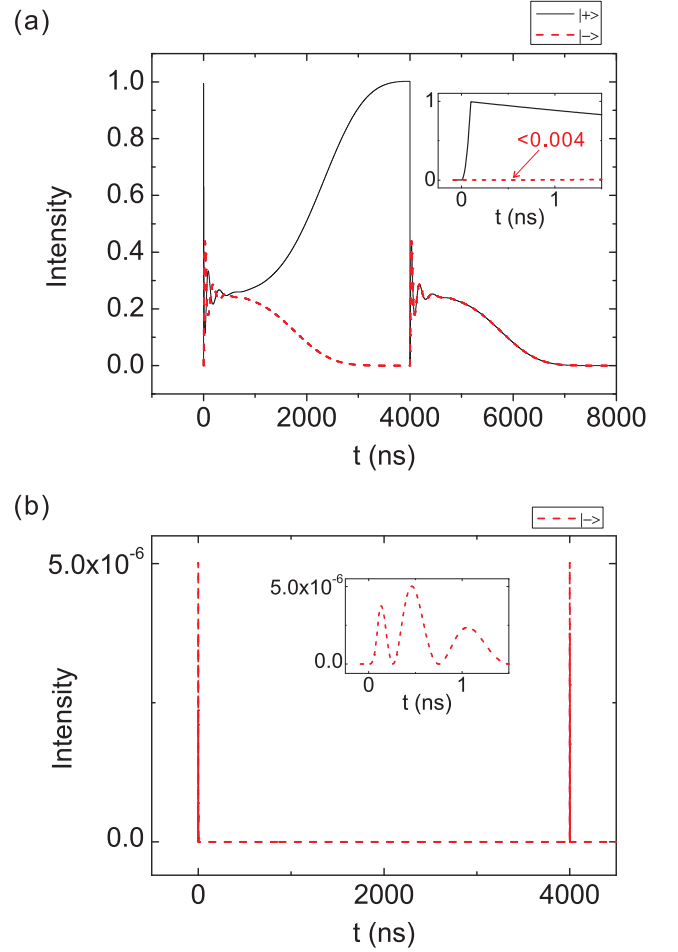


FIG. 3: (color online). Intensity of the transmitted light of the polarizations $|+\rangle$ (black solid line) and $|-\rangle$ (red dashed line) without the filter (a) and with the filter (b).

between the two paths for the given delay time. A time delay τ_d between the arrival of H and V polarized light would lead to a remarkable intensity for I_- , which can be estimated to be τ_d/t_r . However, for Fig. 3(a) with no filter present, I_- can grow to 0.004 in the first nanoseconds with no delay for either paths. Therefore, it becomes impossible to measure τ_d with sub-picosecond accuracy.

The transmission $I_-(z_2, t)$ with the filter is shown in Fig. 3(b). I_+ is the same as that in Fig. 3(a) which is not shown in Fig. 3(b). Because the filter has wideband absorption, only photons with frequencies far-detuned from the resonance are transmitted. The main fields are totally absorbed by the filter, and only precursors at $t = 0$ and $t = t_0$ remain. For all time scales, at most I_- can grow to 5×10^{-6} in the first nanoseconds after $t = 0$ and $t = t_0$. Because the remaining far-detuned light experiences little phase shift, there is near-perfect interference between the two paths. Therefore, whenever there is an intensity larger than 10^{-5} recorded for I_- , we may infer that there is a time delay between the arrival of H and V polarized light. Moreover, the interference yield the same results when

the first $\text{Nd}^{3+}:\text{YVO}_4$ crystal acts as a two level system, which is the fast light regime.

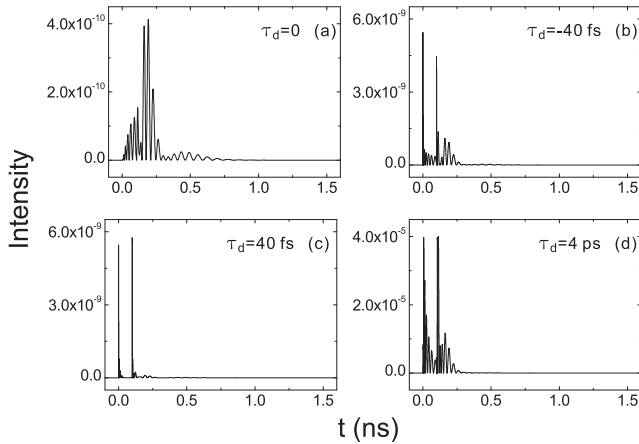


FIG. 4: Intensity of $[-]$ polarized light for $\tau_d = 0$ (a), $\tau_d = -40$ fs (b), $\tau_d = 40$ fs (c) and $\tau_d = 4$ ps (d).

To accurately determine the speed of precursors using this method, let $z_1 = 0.055$ m, $z_2 = 0.08$ m, and $\delta_2 = 1050\delta_1$ which is roughly the inhomogeneous broadening of the Nd^{3+} ions. Thus, the lower AOM in Fig. 2 may not be necessary. The propagation time in the first crystal is $t_1 \approx z_1/v_0 \approx 400$ ps. Notice that z_2 can be much shorter if the crystal has a higher doping level. A time delay τ_d between the H and V polarized light is artificially introduced. Let $E_H(z_2, \omega) = \sqrt{1/2}E(0, \omega)\text{Exp}[ik_1(\omega)z_1]\text{Exp}[i\omega\tau_d]$. This means the H polarized precursors will fall behind (move ahead) of the V polarized light by $|\tau_d|$ for $\tau_d > 0$ ($\tau_d < 0$). The output intensities for the same input pulse with $\tau_d = 0, -40$ fs, 40 fs, 4 ps are shown in Fig. 4(a-d), respectively. Clearly I_- with $|\tau_d| = 40$ fs is much greater than that without delay. The longer the delay, the greater the I_- that can be obtained. Whether the H polarized precursors are faster or slower than the V polarized light has little effect on the output. This is shown in Fig. 4(b) and Fig. 4(c). The sign of τ_d may be experimentally identified by introducing a compensation delay in either path. The probe light intensity can be chosen to be 1 mW in the experiment. Therefore, when I_- is detected with a value over 6 pW, we can conclude that there is a speed difference $\Delta v > v_0/10^4$ for the two paths, which is approximately $\Delta v/v_0 \approx \tau_d/t_1$. With the parameters chosen here, a bound of less than 10^{-4} on the accuracy of the precursors' speed can be experimentally determined.

Note that when t_0 is changed, it only slightly affects the results. This is because only the fast rising and falling edge which contain the wideband frequency components contribute to the precursors. This results from the fact that all the central frequency components were absorbed by the filter.

The highest speed resolution with this scheme is not limited to 10^{-4} which depends on several parameters. The first is the rise time of the input pulse, which is determined by the modulation method. Because $I_- \propto \tau_d/t_r$, the smaller t_r is, the

more sensitive I_- is to τ_d . The faster the signal rises, the harder they can "see" Nd^{3+} in $\text{Nd}^{3+}:\text{YVO}_4$ crystal. The second is the length of the first crystal, z_1 , which determines the transmission time t_1 . Because $\Delta v/v_0 \approx \tau_d/t_1$, for a larger t_1 , the speed difference can be determined more precisely. Third, detectors with better low-intensity responses can resolve a smaller τ_d . Note that the rise time of the detectors is not so important in this scheme because only the maximal intensity is interested rather than the absolute time that the signal rises. Therefore, the accuracy of the measurement can be improved with better experimental conditions. Compared with previous works which determine the speed of information to the accuracy of about 0.1 by directly intensity recording [5, 25], our scheme shall give more accurate measurements.

To summarize, we propose a practical method to compare the propagation speeds of optical precursors in $\text{Nd}^{3+}:\text{YVO}_4$ and pure YVO_4 crystals. This method can determine the speed of the precursor to an accuracy of a given lower-bound. This scheme also can be applied in other systems, such as other rare-earth-ion doped crystals, atom vapors and cold atoms. For cold atoms, the reference speed would be the vacuum speed c .

This work was supported by National Fundamental Research Program, National Natural Science Foundation of China (Grant Nos. 60621064 and 10874162).

-
- [1] A. Einstein, *Ann. Phys.* **17**, 891 (1905).
 - [2] Robert W. Boyd *et al.*, *Science* **326**, 1074 (2009).
 - [3] L. J. Wang *et al.*, *Nature* **406**, 277 (2000).
 - [4] Matthew S. Bigelow *et al.*, *Science* **301**, 200 (2003).
 - [5] Michael D. Stenner *et al.*, *Nature* **425**, 695 (2003).
 - [6] Gunnar Dolling *et al.*, *Science* **312**, 892 (2006).
 - [7] George M. Gehring *et al.*, *Science* **312**, 895 (2006).
 - [8] A. Sommerfeld, *Ann. Phys.* **44**, 177 (1914).
 - [9] L. Brillouin, *Ann. Phys.* **44**, 203 (1914).
 - [10] An English translation of [8, 9] can be found in a book by L. Brillouin, *Wave Propagation and Group Velocity* (Academic Press, New York, 1960).
 - [11] R. Albanese *et al.*, *J. Opt. Soc. Am. A* **6**, 1441 (1989).
 - [12] S.-H. Choi *et al.*, *Phys. Rev. Lett.* **92**, 193903 (2004).
 - [13] Heejeong Jeong, and Shengwang Du, *Opt. Lett.* **35**, 124 (2010).
 - [14] J. F. Chen *et al.*, *Phys. Rev. Lett.* **104**, 223602 (2010).
 - [15] J. Aaviksoo *et al.*, *Phys. Rev. A* **44**, R5353 (1991).
 - [16] Éric Falcon *et al.*, *Phys. Rev. Lett.* **91**, 064502 (2003).
 - [17] Heejeong Jeong *et al.*, *Phys. Rev. Lett.* **96**, 143901 (2006).
 - [18] Shengwang Du *et al.*, *Opt. Lett.* **33**, 2149 (2008).
 - [19] William R. LeFevre *et al.*, *Phys. Rev. A* **79**, 063842 (2009). Heejeong Jeong *et al.*, *Phys. Rev. A* **79**, 011802(R) (2009). Bruno Macke *et al.*, *Phys. Rev. A* **80**, 011803(R) (2009). J. F. Chen *et al.*, *Phys. Rev. A* **81**, 033844 (2010).
 - [20] Dong Wei *et al.*, *Phys. Rev. Lett.* **103**, 093602 (2009).
 - [21] Hugues de Riedmatten *et al.*, *Nature* **456**, 773 (2008).
 - [22] S. R. Hastings-Simon *et al.*, *Phys. Rev. B* **77**, 125111 (2008).
 - [23] Mikael Afzelius *et al.*, *J. Lumin.* **130**, 1566 (2010).
 - [24] Michael Fleischhauer *et al.*, *Rev. Mod. Phys.* **77**, 633 (2005).
 - [25] Michael D. Stenner *et al.*, *Phys. Rev. Lett.* **94**, 053902 (2005).